DINAME 2019 - Proceedings of the XVIII International Symposium on Dynamic Problems of Mechanics,
M.A. Savi, T.G. Ritto and W.M. Bessa (Editors), ABCM, Buzios, RJ, Brazil, March 10th to 15th, 2019

Vortex Induced Motions of a Moored Monocolumn Platform

Brunno Aviles Pesce [1], Éverton Lins de Oliveira [2] and Celso Pupo Pesce [1]

[1] Offshore Mechanics Laboratory, Naval and Ocean Engineering Graduate Program

[2] Dynamics and Control Laboratory, Mechanical Engineering Graduate Program

Escola Politécnica, University of São Paulo, São Paulo, Brazil

Abstract: This paper deals with the dynamics of an offshore moored monocolumn platform subject to ocean currents. Floating Production Storage Offloading (FPSO) offshore platforms of the monocolumn type are enormous structures designed as oil processing facilities to operate in deep and very deep waters. Usually of circular shape, such structures are moored to the seabed. Being bluff bodies, they are subjected to Vortex Induced Motions (VIM) or simply Flow Induced Motions (FIM) caused by the current flow. In the last decade, a plethora of research studies has been dedicated to this topic, approached either from the numerical or from the experimental side, this latter through small-scale models tested in water channel or ocean basis facilities. The present research work proposes a 5dof reduced order model, in which analytical mechanics guides the derivation of the governing dynamic equations of the platform on the horizontal plane, forced through hydrodynamic forces caused by the wake. The hydrodynamic forcing is dynamically represented with a 2dof phenomenological model, based on the coupling of two van der Pol oscillators, commonly referred to as wake-oscillator models. The reduced order model is applied to a case study, the MonoBR-GoM platform, supposed moored in 500m deep water through chains in catenary configuration. The dynamic response is analyzed and effects on motions due to the nonlinear restoring mooring forces are investigated.

Keywords: monocolumn platform, vortex-induced motion, mooring system, reduced order model, wake-oscillators

INTRODUCTION

Offshore oil and gas exploitation in deep and very deep waters rely on the use of FPSO (Floating, Production, Storage and Offloading) platforms, moored to the seabed in a variety of forms, from simple chain catenary configurations to mixed mooring lines, which includes chains, cables (polypropylene and steel), mounted in taut leg configurations; see, e.g., Faltinsen (1990) or Chryssostomidis and Liu (2011). Usually the FPSO has a ship shaped hull especially designed for the moored offshore activity, with a whole chemical processing plant on deck. Another kind of FPSO, the so-called MPSO (Monocolumn Production, Storage and Offloading system; Gonçalves et al, 2010b), or simply monocolumn platform, is characterized by a large diameter cylindrical hull that pierces the free surface. Existing unities or designs may have a moon-pool inside, an internal pool through which risers and umbilical cables are connected to the wellheads and subsea equipment.

Figure 1 – Monocolumn platforms. Left: MonoBR-GoM, (Nishimoto et al, 2010), with a moon-pool. Right up: FPSO Sevan[1] Hummingbird; bottom: FPSO Sevan Piranema, (Gonçalves et al, 2010b).

Figure 1 shows examples of MPSO existing designs or operating unities. On the left, the MONOBR-GoM platform (Nishimoto et al, 2010), designed to operate in the Gulf of Mexico, by adapting the original MonoBR concept. This

[1] Sevan Marine company

concept exhibits a moon-pool. On the right, two existing unities in full operation, the Sevan[1] monocolumn platforms (Saad et al, 2009, Gonçalves et al, 2010b). In those cases, the platform is not equipped with moon-pool. The main feature of the cylindrical platform is its somewhat low response heave motion to incident waves, beneficial to operational conditions and to loadings on risers and umbilicals (Gonçalves et al, 2010). Particularly, the dynamics of the water column inside the moon-pool, if properly tuned, mitigates even more the heave motion of the platform (Nishimoto et al, 2010, Gonçalves et al, 2010b).

On the other hand, the cylindrical shape characterizes a bluff body, prone to vortex-induced vibrations, eventually caused by ocean currents. In fact, shedding vortices phenomena may take place. However, the monocolumn platform hull is usually a low-aspect ratio circular cylinder, so that the common vortex-shedding phenomenon from long rigid cylinders, usually related to the so-called Karman-street, may be strongly affected by three-dimensional vortex structures emanated from the lower face of the cylindrical hull. Such a matter has been investigated extensively in the recent years, both experimentally or numerically (Fujarra et al, 2007, Fujarra et al, 2012, Gonçalves et al, 2009, 2010a, 2012a,b, 2013, 2015, 2018). Such a complex three-dimensional flow impairs not only computational fluid dynamics approaches as creates extra obstacles in pursuing reliable and simple empirical hydrodynamic models. However, it has been shown that for aspect ratios of order one, some regularity in the wake do exist (Gonçalves et al, 2018). Essentially, that has been the reason for the use of phenomenological models, the so-called wake-oscillator models, to face the VIM of monocolumns, irrespective their restrictive assumptions (Rosetti et al, 2009; Lacerda et al, 2009; Rosetti et al, 2011; Lacerda 2011). In particular, Rosetti et al, 2011, present an extensive discussion, with experimental comparisons, on an ad-hoc 2dof phenomenological model, applied to represent the VIM of monocolumn platforms.

In fact, such an approach had been used since the 1970's (Iwan and Blevins, 1974), but in the classic rigid cylinder 1dof VIV (Vortex-Induced Vibration) context. Since VIV is an auto-excited and auto-regulated phenomenon, i.e., a post-critical response after a Hopf bifurcation, van der Pol, Rayleigh or Landau oscillators have had their coefficients experimentally adjusted to represent the VIV phenomenon; see, e.g., Aranha, 2004, for a first principle derivation of a Landau wake-oscillator from the Navier-Stokes equations. After Fachinetti et al. 2004 revisited the phenomenological approach for the 1dof VIV, some effort has been put on wake-oscillators, trying to improve them to represent the so-called 'lower-branch response' (Ogink and Metrikine, 2010). More recently, Franzini and Bunzel (2018) extended the Ogink and Metrikine's model to consider the 2dof situation. In the context of VIM we chose to use the already existing model by Rosetti et al (2009), with the coefficients calibrated according to Postnikov et al. (2016), on an ad-hoc basis.

Guided by the formalism of analytic mechanics, the dynamic equations that govern the motion of monocolumn platform on the horizontal plane are derived. The nonlinear mooring lines restoring forces are worked out analytically, following a previous derivation by Pesce et al, 2018. Then, taking the MonoBR-GoM platform as a case study, some dynamic simulations are performed. The effect of mooring forces linearization is assessed and exemplified, by varying the ocean current intensity. Some examples are also shown, concerning effects caused by the current direction.

REDUCED ORDER MATHEMATICAL MODEL

A 5dof reduced-order model is presented below for the problem under discussion. The model considers the motion of the platform, taken as a rigid body, on the horizontal plane only (3dof). The equations of motions are derived from the classic Lagrangian formalism. Hydrodynamic and mooring line restoring forces on the horizontal plane are taken as generalized forces.

The generalized mooring line restoring forces are modeled in a quite general way, through the formalism of analytical mechanics, following the derivation by Pesce et al, 2018. Such a derivation permits to consider rather distinct mooring configurations, taking nonlinearities into account. It is somewhat restrictive though, since restoring forces are considered to be function of position only, in a quasi-static approach. Effects associated to the mooring line system dynamics are not considered in this model, what would include mooring line damping. This issue deserves a proper discussion that will be left for a further work.

The hydrodynamic forces may be divided in two kinds: (i) the inertial ones, represented through the well-known concept of added mass tensor; (ii) those related to the vortex shedding phenomenon, here represented through a phenomenological approach, considering two wake-oscillators, of the van der Pol type, corresponding to forcing in the direction of the current (in-line direction) and transversal to it (crosswise direction). These two oscillators involve two additional degrees of freedom, that summed up to the three degrees of freedom of the platform on the horizontal plan, totalize the 5dof of the reduced order model. In the sequel, the governing equations for the dynamic of the platform are established.

The equations of motions on the horizontal plane

The platform is considered a rigid body, restricted to move on the horizontal plane only. A fixed Cartesian reference frame (O,X,Y) - supposed inertial - and a non-inertial one (A,ξ,η), fixed to the body, are depicted in Figure 2. The *yaw* motion is indicated by the generalized coordinate ψ. Let $\mathbf{q}=\begin{bmatrix} x & y & \psi \end{bmatrix}^T$ be the generalized coordinate vector, where x, y and ψ are named simply *surge*, *sway* and *yaw* motions, no ambiguity implied since the platform is circular.

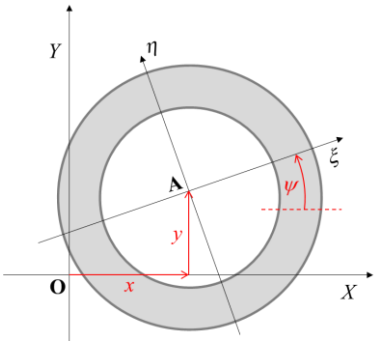

Figure 2 – Coordinates and general definitions.

The Lagrange equations of motion then read:

$$\frac{d}{dt}\left(\frac{\partial T}{\partial \dot{\mathbf{q}}}\right)-\frac{\partial T}{\partial \mathbf{q}}=\mathbf{Q}^m+\mathbf{Q}^v\,, \tag{1}$$

where T is the kinetic energy function of the system, including terms associated to the platform itself and to the internal and the surrounding fluid; $\mathbf{Q}^m=\left[Q_j^m\right]$ and $\mathbf{Q}^v=\left[Q_j^v\right]$; $j=1,2,3$, are, respectively, the generalized forces corresponding to the restoring mooring forces and to the hydrodynamic forces associated to vortex shedding phenomena effects. Let $\mathbf{M}=\mathbf{M}_p+\mathbf{M}_a$ be the (3×3) mass matrix, where the subscript *p* refers to the platform and the subscript *a* to the classic added mass tensor concept. Then the kinetic energy may be put in the following form:

$$T=\frac{1}{2}\dot{\mathbf{q}}^T\mathbf{M}\dot{\mathbf{q}}\,, \tag{2}$$

In the general case, the mass matrix is a full matrix, such that the generalized coordinates couple inertially. However, in the present case, being $A\equiv G$ the center of mass and assuming the body axisymmetric with respect to a vertical axis *Gz*, the mass matrix reduces to a simple diagonal form:

$$\mathbf{M}=\mathbf{M}_p+\mathbf{M}_a=\begin{bmatrix}M&0&0\\0&M&0\\0&0&I\end{bmatrix}+\begin{bmatrix}M_a&0&0\\0&M_a&0\\0&0&I_a\end{bmatrix}, \tag{3}$$

where M is the mass of the platform, itself, I its moment of inertia around Gz and M_a and I_a are the corresponding added mass terms. Note that, usually, the added mass tensor is calculated in the body-reference frame and transformed to the inertial one through a simple matrix rotation operation. However, due to the assumed symmetry, the added mass tensor is invariant with respect to rotations around vertical axes. In other words, $M_a=M_{\xi\xi}=M_{\eta\eta}$. On the other hand, free surface effects may come into play. In fact, in the case of floating bodies, the added mass tensor depends on the frequency of oscillation. However, the system is characterized by a huge inertia and low restoring forces on the horizontal plane, so exhibiting very-low natural frequencies. In resonant conditions, very-low oscillation frequencies are then expected, such that asymptotic values at null frequency may be taken for the added mass; see e.g., Pesce et al, 2018. Notice also that, in the case of a moon-pool, the mass of water inside it has to be considered included in M_a. Moreover, recalling the circular shape and neglecting hull appendices effects, the added moment of inertia, in the classic sense, may be assumed to be null; i.e., $I_a\cong0$. Summarizing, in the present work

$$M_a=C_a\left(\rho\frac{\pi D^2}{4}H\right)+M_{mp};\;\; I_a=0\,, \tag{4}$$

where C_a is the added mass coefficient for a regular cylinder of external diameter D and draught (height) H; and M_{mp} is the mass of water inside the moon-pool. For simplicity, the mass of water inside the moon-pool is taken as constant. In the real environment, the moon-pool water column may resonate, driven by incident ocean waves and by the resulting heave motion of the platform, what would turn the derivation of the equation of motions much more complex. The extended form of the Lagrange equations, that takes into account mechanical systems with variable mass, derived by Pesce, 2003 (see also Pesce et al 2006), should be applied in this case.

Under the above set of simplifying assumptions and recalling that $A\equiv G$ was taken as the center of mass, the equations of motions (1) will then appear in a rather simple form,

$$\mathbf{M}\ddot{\mathbf{q}}=\mathbf{Q}^m+\mathbf{Q}^v\,. \tag{5}$$

Mooring forces on the horizontal plane

We follow closely the derivation presented in Pesce et al (2018). In that paper, a generic mooring system is considered and a model for the corresponding generalized restoring forces on the horizontal plane is constructed geometrically and with the help of analytical mechanics. Figure 3 shows a sketch, where a generic mooring line is considered, projected onto the horizontal plane. $\mathbf{P}_i$, i=1,...,N, are the projections of the hanging points in the platform hull (fairleads) on that plane; $\mathbf{A}_i = \left[x_{A_i} \quad y_{A_i}\right]^T$, i=1,...,N, are the projections of the anchors; $r_i = \overline{\mathbf{A}_i\mathbf{P}_i} = \left|\mathbf{A}_i - \mathbf{P}_i\right|$ are the distances between $\mathbf{P}_i$ and $\mathbf{A}_i$; $R_i = \overline{\mathbf{P}_i\mathbf{A}} = \left|\mathbf{P}_i - \mathbf{A}\right| = const$ are the distances between $\mathbf{P}_i$ and $\mathbf{A}$ and $\beta_i = const$ is the angle between $\overline{\mathbf{P}_i\mathbf{A}}$ and the body axis $\mathbf{A}\xi$. In the present case $R_i = R$, i=1,...,N.

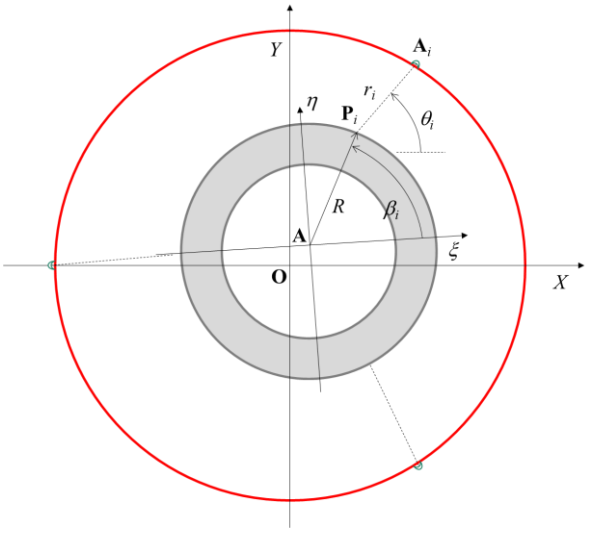

Figure 3 – Mooring system sketch and general definitions; adapted from Pesce and Simos, 2018.

The generalized restoring mooring forces may then be written (Pesce et al, 2018)

$$Q_j^m = \sum_{i=1}^{N} \mathbf{F}_i^T \frac{\partial \mathbf{P}_i}{\partial q_j} = \sum_{i=1}^{N} f_i\left(r_i\right)\mathbf{e}_i^T \frac{\partial \mathbf{P}_i}{\partial q_j};\ \ j = 1,2,3;\ \ i = 1,..,N\,, \tag{6}$$

where

$$\mathbf{e}_i = \frac{\left(\mathbf{A}_i - \mathbf{P}_i\right)}{\left|\mathbf{A}_i - \mathbf{P}_i\right|} = \frac{\left(\mathbf{A}_i - \mathbf{P}_i\right)}{r_i} = \left[\cos\theta_i \quad \sin\theta_i\right]^T;\ \ i = 1,..,N\,, \tag{7}$$

are unit director vectors on the horizontal plane and

$$\mathbf{F}_i = \mathbf{F}_i\left(r_i\right) = f_i\left(r_i\right)\mathbf{e}_i;\ \ i = 1,..,N\,, \tag{8}$$

are the horizontal components of tractions provided by each one of the mooring lines. The restoring force intensities are supposed to be nonlinear functions of position only, in the form $f(r_i)$, no friction or viscous effects considered, in a quasi-static and simplified point of view. Moreover, since each fair-lead position on the horizontal plane,

$$\mathbf{P}_i = \left[x + R_i\cos\left(\psi + \beta_i\right) \quad y + R_i\,\mathrm{sen}\left(\psi + \beta_i\right)\right]^T, \tag{9}$$

is a function of the generalized coordinate vector $\mathbf{q} = \left[x \quad y \quad \psi\right]^T$, the generalized restoring mooring force vector may be also written as a function $\mathbf{Q}^m = \mathbf{Q}^m(\mathbf{q};\Pi)$, where $\Pi = \left\{\left(\mathbf{A}_i \quad R_i \quad \beta_i\right); i = 1,..,N\right\}$ is a set of geometrical parameters. Then, as the restoring forces are supposed strictly dependent on position, a local stiffness matrix may be constructed (Pesce et al, 2018), in the form:

$$\mathbf{K}\left(\mathbf{q};\Pi\right) = -\left[\frac{\partial Q_j}{\partial q_k}\right], \tag{10}$$

leading to

$$\mathbf{K}(\mathbf{q};\Pi) = \begin{bmatrix} k_{xx} & k_{xy} & k_{x\psi} \\ k_{xy} & k_{yy} & k_{y\psi} \\ k_{x\psi} & k_{y\psi} & k_{\psi\psi} \end{bmatrix}, \tag{11}$$

where, the diagonal terms read

$$k_{xx} = \sum_{i=1}^{N}\left(k_i \cos^2(\theta_i) + \bar{k}_i \operatorname{sen}^2(\theta_i)\right)$$

$$k_{yy} = \sum_{i=1}^{N}\left(k_i \operatorname{sen}^2(\theta_i) + \bar{k}_i \cos^2(\theta_i)\right) \quad , \tag{12}$$

$$k_{\psi\psi} = \sum_{i=1}^{N}\left(k_i R_i^2 \operatorname{sen}^2(\psi + \beta_i - \theta_i)\right) + \sum_{i=1}^{N}\bar{k}_i R_i^2\left(\cos^2(\psi + \beta_i - \theta_i) + \frac{r_i}{R_i}\cos(\psi + \beta_i - \theta_i)\right)$$

and the off-diagonal ones,

$$k_{xy} = k_{yx} = \sum_{i=1}^{N}\left(k_i - \bar{k}_i\right)\operatorname{sen}(\theta_i)\cos(\theta_i)$$

$$k_{x\psi} = k_{\psi x} = -\sum_{i=1}^{N}\left(k_i R_i \cos(\theta_i)\operatorname{sen}(\psi + \beta_i - \theta_i)\right) + \sum_{i=1}^{N}\left(\bar{k}_i R_i \operatorname{sen}(\theta_i)\cos(\psi + \beta_i - \theta_i)\right), \tag{13}$$

$$k_{y\psi} = k_{\psi y} = -\sum_{i=1}^{N}\left(k_i R_i \operatorname{sen}(\theta_i)\operatorname{sen}(\psi + \beta_i - \theta_i)\right) + \sum_{i=1}^{N}\left(\bar{k}_i R_i \cos(\theta_i)\cos(\psi + \beta_i - \theta_i)\right)$$

being $f_i' = df_i / dr_i = k_i(r_i)$ the 'tangent stiffness' of each line i and $\bar{k}_i(r_i) = f_i(r_i)/r_i$ its respective 'string stiffness', associated to the 'tensioning state'. A thorough discussion on the effects of pre-tensioning, offset and heading of the platform on the mooring stiffness matrix and on natural periods and corresponding vibration modes may be also found in Pesce et al, 2018. Notice that this model is quite general, being applicable for any mooring system, provided the functions $f_i(r_i);\ i = 1,..,N$ are known. See an application to standard catenary mooring lines in Pesce et al, 2018.

Phenomenological model and hydrodynamic forces

Considering Figure 4, we follow Ogink e Metrikine (2010) to write the hydrodynamic forces in the inertial frame. Let V be the free stream velocity, here supposed aligned with the axis *Ox*. Let *U* be the instantaneous relative velocity of the stream with respect to the center of the body, being U_x and U_y their projections on the axes *x* and *y*. Define F_L and F_D as 'lift' and 'drag' forces, respectively, the former perpendicular to *U* and the latter aligned with *U*. F_{Vx} and F_{Vy} are the components of the hydrodynamic forces in the directions *x* and *y*, respectively. β is the angle between the directions of U and V.

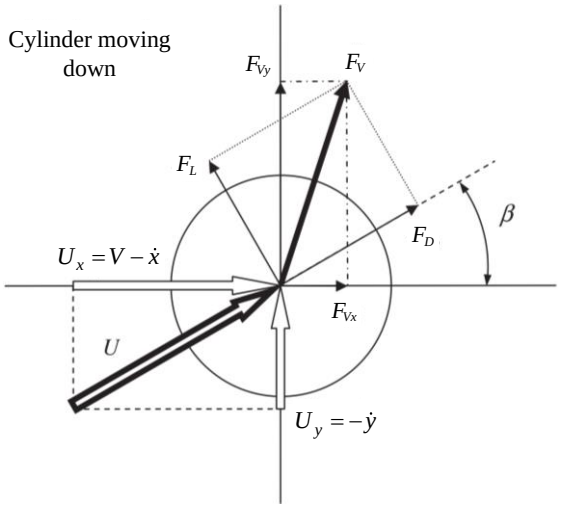

Figure 4 – Forces diagram; adapted from Ogink and Metrikine (2010). Cylinder moving left and down.

Then, from (Ogink and Metrikine, 2010) and (Slingsby, 2015):

$$F_{Vx} = \frac{1}{2}\rho DLC_x V^2;\ F_{Vy} = \frac{1}{2}\rho DLC_y V^2$$

$$C_x = \left(C_D U_x - C_L U_y\right)\frac{U}{V^2};\ C_y = \left(C_D U_y + C_L U_x\right)\frac{U}{V^2}, \tag{14}$$

$$U_x = V - \dot{x};\ U_y = -\dot{y};\ U = \sqrt{U_x^2 + U_y^2}$$

where C_x and C_y are hydrodynamic coefficients in their respective directions (*surge* and *sway*). On the other hand, F_{Vx} e F_{Vy} may be written,

$$\begin{aligned} F_{Vx} &= F_D\cos\beta - F_L\sin\beta;\;\; F_{Vy} = F_D\sin\beta + F_L\cos\beta \\ \cos\beta &= U_x/U;\;\; \sin\beta = U_y/U \end{aligned}. \tag{15}$$

Therefore,

$$F_{Vx} = \frac{1}{2}\rho DH\left(C_D U_x - C_L U_y\right)U;\;\; F_{Vy} = \frac{1}{2}\rho DH\left(C_D U_y + C_L U_x\right)U\,, \tag{16}$$

and the corresponding generalized hydrodynamic force vector turns out to be

$$\mathbf{Q}^v = \frac{1}{2}\rho DHU\left[\left(C_D U_x - C_L U_y\right)\;\;\left(C_D U_x - C_L U_y\right)\;\;0\right]^T. \tag{17}$$

The wake oscillator model

Following Rosetti et al (2009) and Postinikov et al (2016), we write two van der Pol oscillators, aligned with in-line and cross-wise directions, in the form:

$$\begin{aligned} \ddot{w}_x + \varepsilon_x\omega_s\left(w_x^2 - 1\right)\dot{w}_x + 4\omega_s^2 w_x &= \frac{A_x}{D}\ddot{x} \\ \ddot{w}_y + \varepsilon_y\omega_s\left(w_y^2 - 1\right)\dot{w}_y + \omega_s^2\dot{w}_y &= \frac{A_y}{D}\ddot{y} \end{aligned}, \tag{18}$$

where $\mathbf{w} = \left[w_x \quad w_y\right]^T$ is a hidden variable vector that phenomenologically emulates the wake dynamics; ε_x and ε_y are damping parameters and $\omega_s = 2\pi S_t\left(V/D\right)$ is the shedding frequency, being S_t a characteristic value of the Strouhal number for the low aspect ratio cylinder case. Notice that the in-line wake oscillator vibrates with twice the frequency corresponding to the cross-wise one. This is a common ad-hoc assumption that comes from well-known experimental observations, according to which the fundamental harmonic of drag forces pulsates twice as faster as the lift forces' one. The terms on the r.h.s of Eq. (18) represent the coupling between the wake oscillators and the body equations of motion. According to Fachinetti et al (2004), coupling through inertial terms are recommended, despite original models apply velocity terms coupling; see, e.g., Iwan and Blevins (1974). The inertial coupling has been followed since, by a number of authors, as Ogink and Metrikine (2010) or Franzini and Bunzel (2018). The coefficients $(\varepsilon_x, \varepsilon_y)$ and (A_x, A_y) are hereinafter calibrated from experiments (Rosetti et al, 2009, 2011) and from CFD simulations (Postinikov et al, 2016).

Finally, the generalized wake forces in Eq. (17) are computed by determining the lift and drag coefficients as functions of $\mathbf{w} = \left[w_x \quad w_y\right]^T$ (Postinikov et al, 2016), (Rosetti et al, 2009), in the form,

$$C_L = \frac{C_{L0}}{2}w_y;\;\; C_D = C_{D0}\left(1 + Kw_y^2\right) + \frac{C_{D0}^f}{2}w_x\,, \tag{19}$$

where C_{L0} and C_{D0} are, respectively, the lift and drag coefficients for a fixed cylinder, C_{D0}^f is a weighting coefficient for the oscillation amplitude of the drag and K is a constant experimentally determined (Rosetti et al, 2009).

The coupled model

Gathering Eqs. (5 - 6) and (14 -19), the 5dof reduced order model may be written in the following form:

$$\tilde{\mathbf{M}}\ddot{\tilde{\mathbf{q}}} = \tilde{\mathbf{Q}}_c + \tilde{\mathbf{Q}}_{nc}\,, \tag{20}$$

where, on the l.h.s., $\tilde{\mathbf{M}} \in \Re^{5x5}$ and $\tilde{\mathbf{q}} \in \Re^5$ are, respectively, the augmented inertia matrix and generalized coordinate vector; and on the r.h.s., $\tilde{\mathbf{Q}}_c \in \Re^5$ and $\tilde{\mathbf{Q}}_{nc} \in \Re^5$ are, respectively, conservative and non-conservative generalized force vectors. Eq. (21) provides their respective forms explicitly.

$$\tilde{\mathbf{M}} = \begin{bmatrix} M + M_a & 0 & 0 & 0 & 0 \\ 0 & M + M_a & 0 & 0 & 0 \\ 0 & 0 & I & 0 & 0 \\ -\dfrac{A_x}{D} & 0 & 0 & 1 & 0 \\ -\dfrac{A_y}{D} & 0 & 0 & 0 & 1 \end{bmatrix};\;\; \tilde{\mathbf{q}} = \begin{bmatrix} \mathbf{q} \\ \mathbf{w} \end{bmatrix} = \begin{bmatrix} x \\ y \\ \psi \\ w_x \\ w_y \end{bmatrix};\;\; \tilde{\mathbf{Q}}_c = \begin{bmatrix} \mathbf{Q}^m \\ -4\omega_s^2 w_x \\ -\omega_s^2 w_y \end{bmatrix};\;\; \tilde{\mathbf{Q}}_{nc} = \begin{bmatrix} \mathbf{Q}^v \\ -\varepsilon_x\omega_s\left(w_x^2 - 1\right)\dot{w}_x \\ -\varepsilon_y\omega_s\left(w_y^2 - 1\right)\dot{w}_y \end{bmatrix}. \tag{21}$$

Note that nonlinearities in Eq. (20) are present in $\tilde{\mathbf{Q}}_c$, through the mooring forces $\tilde{\mathbf{Q}}^m$, as well as in $\tilde{\mathbf{Q}}_{nc}$, both, in $\tilde{\mathbf{Q}}^v$ and in the van der Pol damping terms.

A CASE STUDY

The MonoBR-GoM platform has been taken as a case study. Table 1 shows its main characteristics. The platform is supposed to me moored in 500m deep waters. Figure 5 shows a sketch of a possible mooring arrangement, with 12 mooring lines, clustered around three main directions, at $(\pm\pi/3;\pi)$. For simplicity, mooring lines are supposed to be composed by chains and installed in simple catenary configurations; Table 2. Notice that, in the actual design, the mooring lines are mixed ones (chain - polypropylene cable – chain - steel cable) linked one to another in a taut leg configuration, in 1800m deep water. For the simple adopted catenary configuration, the needed nonlinear relation $f_i(r_i)$ may be written analytically in an inverse form as (Pesce et al, 2018),

$$\frac{r_i(f_i)}{L_i} = 1 - \frac{f_i}{\gamma_i L_i}\left[\left(\frac{1+2\,f_i/\gamma_i z_{fi}}{\left(f_i/\gamma_i z_{fi}\right)^2}\right)^{\frac{1}{2}} - \ln\left(1+\frac{\gamma_i z_{fi}}{f_i}+\left(\frac{1+2\,f_i/\gamma_i z_{fi}}{\left(f_i/\gamma_i z_{fi}\right)^2}\right)^{\frac{1}{2}}\right)\right], \tag{22}$$

where L_i and γ_i are, respectively, the total mooring line length and the immersed weight per unit length and z_{fi} is the distance of the fairlead from the bottom. For comparison sake, cases have been run also supposing a linear restoring system, taking a mooring stiffness matrix calculated from Eq. (11-13) at the neutral equilibrium position, i.e., $\mathbf{K}_0 = \mathbf{K}(\mathbf{0};\Pi)$. Notice that such a stiffness matrix reduces to a diagonal form due to symmetry, so that coupling due to mooring restoring forces is null by construction in this case; see Pesce et al (2018) for a deeper discussion on this matter.

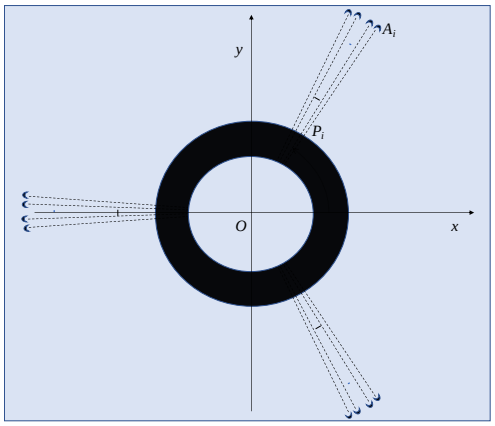

Figure 5 – Sketch of the monocolumn platform mooring system.

The simulations were performed in a MATLAB / Simulink® environment, by numerically integrating the equations of the coupled model in state space form. For the integration, a fixed time step of 0.1 seconds was used, applying the Runge-Kutta method of 4th order. Wake oscillator parameters are given in Table 3. Two current incidence angle conditions were taken to illustrate the reduced order model simulation, both aligned with the global axis *Ox*. The first one assumes that the current acts in the positive direction, from left to right, at $\alpha = 0$. The second one, in the opposite direction, from right to left, at $\alpha=\pi$. Oblique incidences are left for further analyses, to be presented in another paper.

Table 1 – MonoBr-GoM main particulars and general parameters.

Draught, H (m)	39.50
Diameter, D (m)	100.0
Mass, M (t)	262000.0
Added mass coefficient, C_a	1.0
Mass of water in moon-pool, M_{mp} (t)	67447.0
Density of water, $\rho\left(\mathrm{t/m^3}\right)$	1.025

Table 2 – Mooring system: parameters and arrangement at neutral position, $\mathbf{q} = \mathbf{0}$. Catenary chains. Depth 500m.

Immersed weight, γ (kN/m)	1.07
Total length, L (m)	1525.0
Distance of fairlead from anchor, $r\left(f_0\right)$ (m)	1317.0
Horizontal component of pretension, f_0 (kN)	532.83
Number of mooring lines, N	12
Angles of mooring lines in the body frame, β (rad)	[(0.79, 0.96, 1.13, 1.31); (2.88, 3.05, 3.22, 3.40); (-0.79, -0.96, -1.13; -1.31)]

Table 3 – Wake-oscillators parameters; Rosetti et al (2009), Gonçalves et al (2010).

$[\,A_x; A_y\,]$	[12; 6]
$[\,\varepsilon_x; \varepsilon_y\,]$	[0.30; 0.15]
$[\,C_{D0};\ C_{L0};\ C_{D0}^f;\ K\,]$	[0.70; 0.30; 0.10; 0.05]
Strouhal number, S_t	0.078

Figure 6 shows trajectories of the platform center of mass on the horizontal plane, as function of the current velocity, within the range $V \in [0,2;2]\ (\mathrm{m/s})$. Two current directions are exemplified: (i) from left to right, at $\alpha = 0$ and (ii) from right to left, at $\alpha=\pi$. The corresponding reduced velocity, $V_r = 2\pi V/\omega_n D$, is also shown, calculated with $\omega_n = 0,0080\ (\mathrm{rad/s})$, which is the undamped natural frequency in crosswise (*sway*) direction, determined at the neutral position by taking the mooring stiffness matrix $\mathbf{K}_0 = \mathbf{K}(\mathbf{0};\Pi)$. In the legend, 'linear' and 'nonlinear' refer only to the mooring system. The common source of nonlinearities is the wake oscillator. In case (i), $\alpha = 0$, despite amplitudes of crosswise oscillations do not differ too much, in-line oscillations are remarkably distinct for the two mooring system models, making trajectories rather different. As a matter of fact, as in-line oscillations evolve, coupling increases in the nonlinear case, making crosswise oscillations larger than in the linear one. Also noticeable is the larger average offset encountered with the linear mooring system. Moreover, the linear mooring system responses in cases (i) and (ii) are mirrored images of each other, as expected. However, there are strong differences for the nonlinear mooring system model. In fact, the mooring geometry makes the stiffness in the *x*-axis to increase much more rapidly if a negative surge displacement is imposed than in the opposite sense; see Figure 3. Consequently, oscillations are smaller in case (ii). Figure 7 shows the amplitude of motions in both directions, in-line and crosswise, for the two mooring system models, linear and nonlinear. As can be seen, reaffirming the observations made from Fig. 6, the nonlinear restoring coupling ends up amplifying or diminishing the response amplitudes. Also noticeable are the frequencies of oscillation in both directions, which are dependent on the current direction for the nonlinear mooring system model. The stiffer the mooring system, the higher are the oscillation frequencies, as it should be expected. Finally, Figure 8 illustrates time series of the 3dof motions of the platform, including the yaw angle. The linear mooring case is exemplified for case (i), $\alpha = 0$, only, as motion amplitudes are essentially the same for both directions. The nonlinear mooring system model however shows how the mooring restoring forces coupling makes the platform to yaw, even in the absence of yawing moments. In fact, as the current speed increases augmenting the mooring system stiffness, coupling between sway and yaw augments. Such a coupling is larger for case (ii), current flowing left. In the linear mooring case, no yaw motion is excited.

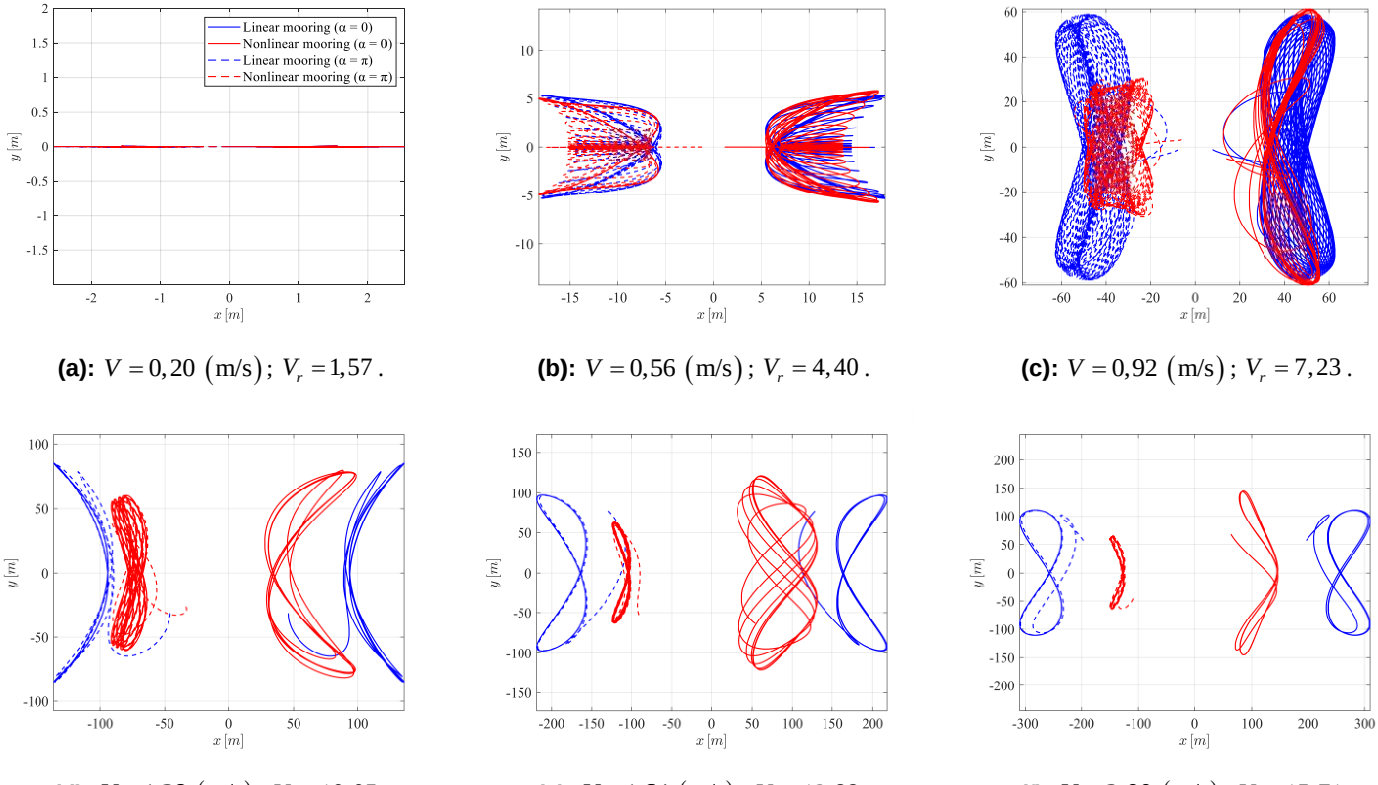

(a): $V = 0,20\ (\mathrm{m/s});\ V_r = 1,57$.

(b): $V = 0,56\ (\mathrm{m/s});\ V_r = 4,40$.

(c): $V = 0,92\ (\mathrm{m/s});\ V_r = 7,23$.

(d): $V = 1,28\ (\mathrm{m/s});\ V_r = 10,05$.

(e): $V = 1,64\ (\mathrm{m/s});\ V_r = 12,88$.

(f): $V = 2,00\ (\mathrm{m/s});\ V_r = 15,71$.

Figure 6 – Center of mass trajectories on the horizontal plane. Current direction: (i) from left to right, α = 0 and (ii) from right to left, α = π. The terms 'linear' and 'nonlinear' in the legend refer only to the mooring system.

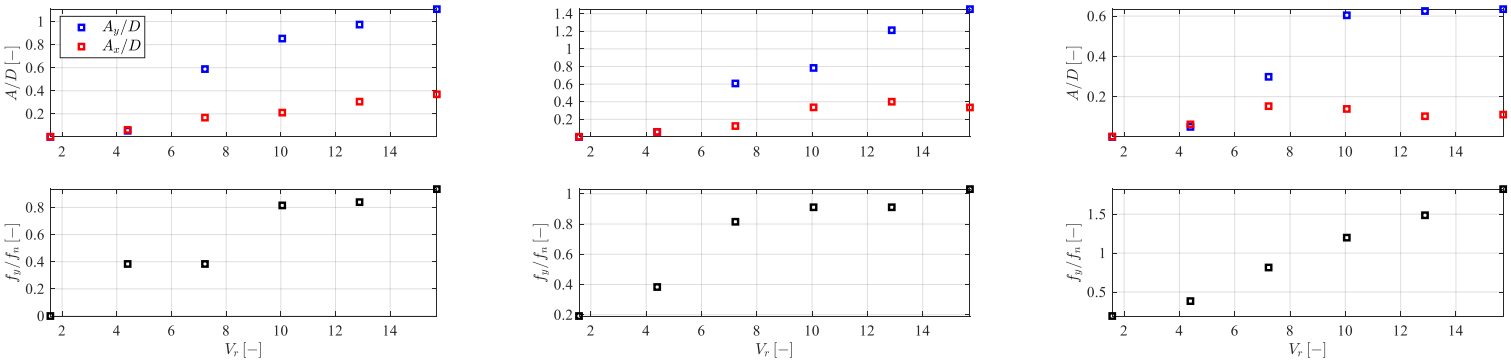

(a) (b) (c)

Figure 7 – Normalized amplitudes and oscillation frequencies, as a function of the reduced velocity. (a): linear mooring model, α = 0; (b): nonlinear mooring model, α = 0; (c): nonlinear mooring model, α = π.

$V = 0{,}56\ (\mathrm{m/s})\ ;\ V_r = 4{,}40\ .$

$V = 1{,}28\ (\mathrm{m/s})\ ;\ V_r = 10{,}05\ .$

$V = 2{,}00\ (\mathrm{m/s})\ ;\ V_r = 15{,}71\ .$

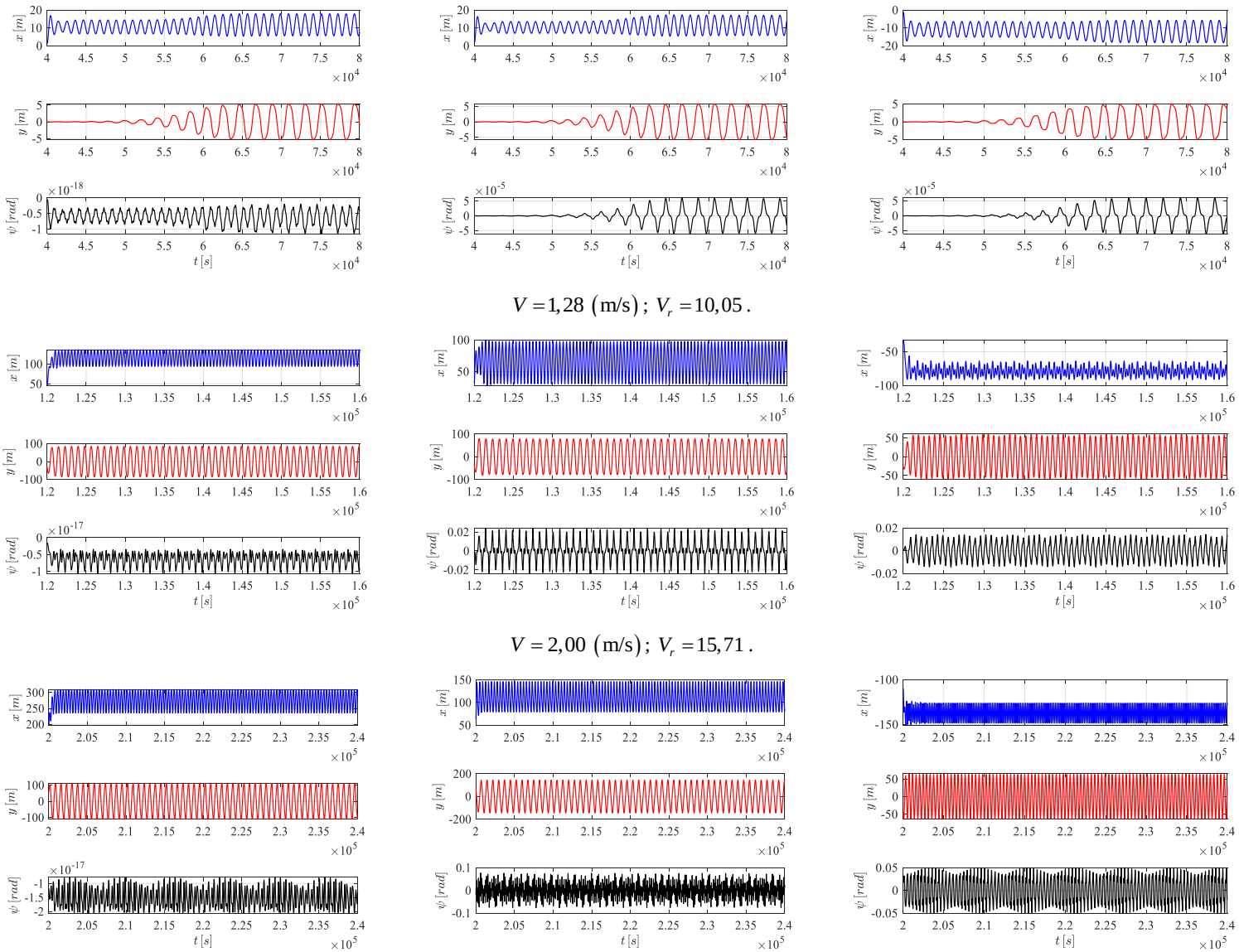

(a) (b) (c)

Figure 8 – Surge, sway and yaw motions; (a): linear mooring model, α = 0; (b): nonlinear mooring model, α = 0; (c): nonlinear mooring model, α = π.

CONCLUSIONS

Vortex Induced Motions of a monocolumn floating platform, subjected to ocean current, have been investigated numerically, through a 5dof reduced order model. Such model considers the motion of the platform on the horizontal plane. Hydrodynamic forces are determined from a phenomenological model, by using a 2dof wake oscillator, a common approach in vortex-induced vibration studies, which has been adopted in recent years for the VIM phenomenon. A nonlinear mooring system restoring forces model, recently developed by Pesce et al (2018), is applied. A case study was done, based on the MonoBR-GoM platform, supposed moored to the seabed in 500m deep water through 12 mooring lines, clustered around three main directions, at $(\pm\pi/3;\pi)$. For simplicity, mooring lines were supposed to be composed by chains and installed in simple catenary configurations. The effects of mooring system nonlinearities on the motions amplitudes, including the coupling with yaw motions, were then illustrated through time-domain simulations for two current directions aligned with an axis of symmetry of the system.

This is an ongoing research. Further investigations about the effects of ocean current oblique incidence on the motion responses are left for further work. Other mooring arrangements and comparisons with experimental data and with existing simulation results are yet to be performed.

ACKNOWLEDGMENTS

The first and the second authors acknowledge PPGEN and PPGEM Graduate Programs for CAPES MSc and PhD scholarships; the third author acknowledges CNPq research grant n. 308990/2014-5. Authors are grateful to Dr. Edgard Malta, Technomar, and to Prof. Kazuo Nishimoto, TPN, USP, for providing the case study data. Tanks also to Profs. M. Savi and T. Ritto for their comprehension and incentive.

REFERENCES

Aranha, J.A.P., 2004, “Weak Three Dimensionality of a Flow around a Slender Cylinder. The Ginzburg-Landau Equation”. Journal of the Brazilian Society of Mechanical Sciences and Engineering, Vol. 26, n.4, p. 355-367.

Chryssostomidis, C. and Liu, Y., 2011, “Design of Ocean Systems”, Department of Mechanical Engineering, Massachusetts Institute of Technology, Massachusetts, USA.

Facchinetti, M.L., de Langre, E. and Biolley, F., 2004, “Coupling of Structure and Wake Oscillators in Vortex-Induced Vibrations”, Journal of Fluids and Structures, Vol. 19, No. 2, pp. 123-140.

Faltinsen, O. M., 1990, “Sea Loads on Ships and Offshore Structures”, Cambridge University Press, New York, USA, 340 p.

Franzini, G. R., Bunzel, L. O., 2018, “A Numerical Investigation on Piezoelectric Energy Harvesting from Vortex-Induced Vibrations with One and Two Degrees of Freedom”. Journal of Fluids and Structures, Elsevier Inc., Vol. 77, pp. 196–212.

Fujarra, A.L.C., Pesce, C.P., Nishimoto, K., Cueva, M.F., 2007, “Non-stationary VIM of Two Mono-Column Oil Production Platforms”. In: BBVIV5, 2007, Costa do Sauípe. 5th Conference on Bluff Body Wakes and Vortex Induced Vibrations.

Fujarra, A.L.C., Rosetti, G.F., Wilde, J. and Gonçalves, R.T., 2012, “State-of-Art on Vortex-Induced Motion: A Comprehensive Survey After More than One Decade of Experimental Investigation”, Proceedings of the ASME 31st International Conference on Ocean, Offshore and Arctic Engineering, Rio de Janeiro, Brazil, pp. 561-582.

Gonçalves, R.T., Franzini, G.R., Rosetti, G.F., Meneghini, J.R., Fujarra, A.L.C., 2015, “Flow Around Circular Cylinders with Very Low Aspect Ratio”. Journal of Fluids and Structures, Vol. 54, p. 122-141.

Gonçalves, R.T., Fujarra, A.L.C., Rosetti, G.F., Nishimoto, K., 2010, “Mitigation of Vortex-Induced Motion (VIM) on a Monocolumn Platform: Forces and Movements”, Journal of Offshore Mechanics and Arctic Engineering, ASME, Vol. 132, No. 4, pp. 1-16.

Gonçalves, R.T., Fujarra, A.L.C., Rosetti, G.F., Nishimoto, K., Cueva, M. and Siqueira, E.F.N., 2009, “Vortex-Induced Motion of a Monocolumn Platform: New Analysis and Comparative Study”, Proceedings of the ASME 28th International Conference on Ocean, Offshore and Arctic Engineering, Honolulu, Hawaii, USA, pp. 343-360.

Gonçalves, R.T., Matsumoto, F.T., Malta E.B., Rosetti, G.F., Fujarra, A.L.C., Nishimoto, K., 2010, “Evolution of the MPSO (monocolumn production, storage and offloading system)”, Marine Systems & Ocean Technology, Vol. 5, No. 1 pp. 43-51.

Gonçalves, R.T., Meneghini, J.R., Fujarra, A.L.C., 2018, “Vortex-Induced Vibration of Floating Circular Cylinders with Very Low Aspect Ratio”. Ocean Engineering, Vol. 154, pp. 234-251.

Gonçalves, R.T., Rosseti, G., Fujarra, A.L.C. and Nishimoto K., 2012, “Experimental Comparative Study on Vortex-Induced Motion (VIM) of a Monocolumn Platform”, Journal of Offshore Mechanics and Arctic Engineering, ASME, Vol. 134, No. 1, pp. 1-15.

Gonçalves, R.T., Rosetti, G.F., Franzini, G.R., Meneghini, J.R., Fujarra, A.L.C., 2013, "Two-degree-of-freedom Vortex-Induced Vibration of Circular Cylinders with Very Low Aspect Ratio and Small Mass Ratio". JOURNAL OF FLUIDS AND STRUCTURES, Vol. 39, p. 237-257.

Gonçalves, R.T., Rosetti, G.F., Fujarra, A.L.C., Nishimoto, K., 2012, "An Overview of Relevant Aspects on Vortex-Induced Motions (VIM) of Spar and Monocolumn Platforms". Journal of Offshore Mechanics and Arctic Engineering, Vol. 134, p. 014501-1-01501-7.

Gonçalves, R.T., Rosetti, G.F., Fujarra, A.L.C., Franzini, G.R., Freire, C.M., Meneghini, J.R., 2012, "Experimental Comparison of Two-degree-of-freedom Vortex-Induced Vibration on High and Low Aspect Ratio Cylinders with Small Mass Ratio". Journal of Vibration and Acoustics, Vol. 134, pp. 061009-1-061009-7.

Iwan, W.D., Blevins, R.D., 1974, "A Model for Vortex Induced Oscillation of Structures", J. Appl. Mechanics, Vol. 41, N. 3, pp. 581-586

Lacerda, T.A.G., 2011, "Estimativa dos Movimentos Induzidos por Vórtices em Plataformas Flutuantes Através de um Oscilador do tipo Van der Pol", Ph.D. Thesis (in Portuguese), Federal University of Rio de Janeiro, Rio de Janeiro, Brazil, 115 p.

Lacerda, T.A.G., Ellwanger, G.B., Siqueira, M.Q. and Siqueira, E.F.N., 2009, "Time Domain Methodology for Vortex-Induced Motion Analysis in Monocolumn Platform", Proceedings of the ASME 28th International Conference on Ocean, Offshore and Arctic Engineering, Honolulu, Hawaii, USA, pp. 717-722.

Lienhard, J.H., 1996, "Synopsis of Lift, Drag, and Vortex Frequency Data for Rigid Circular Cylinders", Technical Extension Service, Washington State University, 64 p.

Maia, A., Masetti, I.Q., Nishimoto, K., Cueva, M. and Cueva D., 2018, "MonoBr e FPSO-BR Novos Desenvolvimentos em Plataformas Flutuantes", Available in: <http://oceanicabr.com> Acessed: August 28th, 2018.

Nishimoto, K., Malta, E.B., Rampazzo, F.P., Matsumoto, F.T., Rateiro, F., Rosetti, G.F., Watai, R.A., "MonoBR-GoM Coupled Analysis", Technical Report, 2010, TPN – Numerical Offshore Tank, Escola Politécnica, University of São Paulo, 105p, (restricted access).

Ogink, R.H.M. and Metrikine, A.V., 2010, "A Wake Oscillator with Frequency Dependent Coupling for the Modeling of Vortex-Induced Vibration", Journal of Sound and Vibration, Vol. 329, No. 26, pp. 5452-5473.

Pesce, C.P., 2003, The Application of Lagrange Equations to Mechanical Systems with Mass Explicitly Dependent on Position, Journal of Applied Mechanics, Vol. 70, pp. 751-756.

Pesce, C.P., Amaral, G.A. and Franzini, G.R., 2018, "Mooring System Stiffness: a General Analytical Formulation with an Application to Floating Offshore Wind Turbines", Proceedings of the ASME 1st International Offshore Wind Technical Conference, San Francisco, Nov 4-7, 2018, IOWTC2018-1040, ASME.

Pesce, C.P., Simos, A.N., 2018, "Class Notes on Dynamics Applied to Ocean Engineering I", Graduate Program in Ocean Engineering, Escola Politécnica, University of São Paulo, São Paulo, Brazil.

Pesce, C.P., Tannuri, E.A., Casetta, L., The Lagrange Equations for Systems with Mass Varying Explicitly with Position: Some Applications to Offshore Engineering, J Brazilian Soc Mech Sciences and Eng, v. XXVIII, 496-504, 2006.

Petrobras, 2018, "Types of Platforms - Monocolumn" Available in: <http://www.petrobras.com.br/infograficos/tipos-de-plataformas/desktop/index.html> Acessed: August 30th, 2018.

Postnikov, A., Pavlovskaia, E. and Wiercigroch, M., 2017, "2DOF CFD Calibrated Wake Oscillator Model to Investigate Vortex-Induced Vibrations", International Journal of Mechanical Sciences, Vol. 27, pp 176-190.

Rosetti, G.F., Gonçalves, R.T., Fujarra, A.L.C., Nishimoto, K., 2011, "Parametric Analysis of a Phenomenological Model for Vortex-Induced Motions of Monocolumn Platforms", J. of the Braz. Soc. of Mech. Sci. & Eng., Vol. 23, N. 2, pp. 139-146.

Rosetti, G., Gonçalves, R.T., Fujarra, A.L.C., Nishimoto, K. and Ferreira, M.D., 2009, "A Phenomenological Model for Vortex-Induced Motions of the Monocolumn Platform and Comparison with Experiments", Proceedings of the ASME 28th International Conference on Ocean, Offshore and Arctic Engineering, Honolulu, Hawaii, USA, pp. 437-444.

Saad, A.C., Vilain, L., Loureiro, R.R., Brandão, M., Machado Filho, R.Z., Lopes, C., Gioppo, H, 2009. "Motion Behaviour of the Mono-Column FPSO Sevan Piranema in Brazilian Waters", Proceedings of the 2009 Offshore Technology Conference, Houston, Texas, USA, 4–7 May 2009, OTC 20139.

Slingsby, M., 2015, "Dynamic Interaction of Subsea Pipeline Spans due to Vortex-Induced Vibrations", Delft University of Technology, M.Sc. thesis, Delft University of Technology, Delf, Netherlands, 162 p.

RESPONSIBILITY NOTICE

The authors are the only responsible for the printed material included in this paper.